International Journal of Mass Spectrometry xxx (2009) xxx–xxx

Contents lists available at ScienceDirect

International Journal of Mass Spectrometry

journal homepage: www.elsevier.com/locate/ijms

Proton transfer mass spectrometry at 11 hPa with a circular glow discharge: Sensitivities and applications

D.R. Hanson*, M. Koppes, A. Stoffers, R. Harsdorf, K. Edelen

Chemistry Department, Augsburg College, 2211 Riverside Ave. Minneapolis, MN 55454, United States

ARTICLE INFO

Article history:
Received 12 September 2008
Received in revised form 30 January 2009
Accepted 31 January 2009
Available online xxx

Keywords:
Proton transfer mass spectrometry
Volatile organic compounds
Glow discharge
Fragmentation

ABSTRACT

The design and testing of a circular glow discharge ion source on a custom built proton transfer mass spectrometer are described. Also, issues important for quantitative measurements of volatile organic compounds using this instrument were investigated. Detailed calibration procedures based on gravimetry are presented, and representative outdoor air data are shown. Calibrations yield a good sensitivity, up to a few Hz/pptv for some compounds, and the detection limit (S/N = 3) is ~100 pptv or better for methanol, acetaldehyde and acetone (5 s sampling time with a 5 s zero). Detection limits are much lower for most other compounds due to high sensitivity and low background. For ions with $m/z > \sim 90$ the background signals are very low and species that appear efficiently at these m/z can be detected at the 10 pptv level in a few seconds. Ion breakup processes for alcohols show that a major product ion of mono-functional alcohols is at 57 u, presumably $C_4H_9^+$. Oxalic acid is an interesting case in that a major product ion appears on an even mass, 46 u, presumably $CO_2H_2^+$. The circular glow discharge source is easy to construct and deploy in proton transfer mass spectrometry studies at ~11 hPa. Continuous use of the system over time periods of many days and stable operation over time periods of months to years between disassembly and cleaning demonstrates its robustness.

1. Introduction

Proton transfer mass spectrometers have been used in a wide variety of experiments for detection of volatile organic compounds (VOCs). Basically, a gas to be analyzed is put into contact with water proton clusters that react with those constituents of high proton affinity. The work of Lindinger et al. [1] has demonstrated the versatility of the proton-transfer-reaction mass spectrometry (PTR-MS) technique: sampling outdoor air, laboratory studies of VOCs, human breath analysis, and analysis of volatile components of food and beverages. A recent review article [2] presents a tailored commercial Lindinger instrument (Ionicon, PTR-MS) for sensitive and accurate detection of VOCs in the atmosphere. They performed detailed calibrations and explored humidity dependencies and showed how PTR-MS data is used to understand atmospheric processes. Hansel et al. [3] and Karl and Guenther [4] are carrying on Lindinger's work and have evaluated the PTR-MS instrument in a wide variety of experimental setups for the measurement of VOCs.

We previously described [5] and evaluated a proton transfer-mass spectrometer (PT-MS, to be distinguished from the PTR-MS) that was operated at a drift tube pressure of 10 Torr (13.2 hPa) employing a radioactive foil (Am-241) ion source. Later, we presented modified drift regions that could be operated at pressures up to 0.8 atm and where the flow of sample gas is transverse to the ion path that allowed for the detection of peroxy radicals and their oxidation products [6]. Here we report on refinements to the drift tube of [5] and the use of a glow discharge ion source. The performance of the refined system is demonstrated through calibrations and example measurements of outdoor air and fragmentation experiments.

The drift tube and ion source pressure are slightly lower in this study, ~10.7 hPa, than in our previous PT-MS work [5], but the high ion production rates of the discharge source leads to a much improved sensitivity. The ion source is a sub-normal (voltage decreases with increasing current) glow discharge at a current of 50–100 μA, [7,8,9]; the commercial PTR-MS uses a normal (voltage is constant with current) glow discharge, characterized by currents in the several mA range (J. deGouw, T. Karl, 2008, private communication).

The soft ionization of proton transfer generally preserves the parent mass M in the product ion $M{\cdot}H^+$ but for a number of compounds this is not true [10,11,12,26] and more work [2] is needed in this area. We present ion breakup processes for a few alcohol species, isoprene, and oxalic acid.

The commercial PTR-MS (Ionicon) measurement for benzene reportedly has no dependence on RH while the modified PTR-MS of Warneke et al. shows a significant RH dependency for benzene and toluene. These instruments have comparable drift tube pressures

* Corresponding author. Tel.: +1 612 330 1620; fax: +1 612 330 1649.
E-mail address: hansondr@augsburg.edu (D.R. Hanson).

1387-3806/$ – see front matter © 2009 Elsevier B.V. All rights reserved.
doi:10.1016/j.ijms.2009.01.021

(2–2.5 hPa) but the former generally has an E/N of 120–140 Td [1] while the latter has been run at 107 Td [14,34]. The RH dependence for several compounds is investigated here.

The performance of the PT-MS is demonstrated with calibrations to illustrate the sensitivity and detection limits of the instrument as well as RH dependencies. Results of PT-MS monitoring of VOCs in outdoor air are presented. Comparisons are made between the present system and the conventional PTR-MS techniques typically operated at 2–2.5 hPa.

2. Experimental details

2.1. Glow discharge, drift tube, sample lines

The ion source and drift tube and associated plumbing are illustrated in Fig. 1.The mass spectrometer is a conventional quadrupole (19 mm rod diameter) that is differentially pumped: one 250 L/s turbopump on the quadrupole and one to three turbopumps on the front chamber where most of the gas load is [5]. The ions are produced in a circularly shaped sub-normal glow discharge [7] in clean air that is humidified to ~3% (100% relative humidity at 1 atm). The discharge takes place between a stainless steel plate (or a step on a different source housing), acting as the anode, and the stainless steel source exit plate (~0.8 mm thick) acting as a cathode. A separation of 6.3 mm is set by a static dissipative (SD) Teflon donut spacer (ID of 3.2 cm) and the glow discharge takes the form of a ring just inside the Teflon spacer; confirmed by visual inspection of the cathode where a slight ion burn in a circular shape was apparent (a few cm diameter). The cathode plate has a small (2–7 mm diameter) hole centered in it through which ions enter the drift tube. The typical discharge current is ~45 μA at a voltage drop of ~380 V: ~3800 V was applied to the anode (MC50, Gamma High Voltage, Ormond Beach, FL), leaving ~3420 V on the source exit plate at the typical operating pressure of 10.7 hPa. Ion source regions of a similar nature have been called hollow cathode or hollow anode types (e.g., [1,2,8,9]) where the discharge takes place near to or inline with the ion exit hole.

Like the ion source in the conventional PTR-MS [1,2], the circular discharge current occurs far from where ions exit the source, yet the circular discharge does not use a secondary chamber to convert unwanted ions to water proton clusters. Thus, the circular glow discharge is easy to construct and deploy and yields a large ion current at a low discharge current. Finally, the conventional PTR-MS ion source takes place in low flow of pure water while the circular discharge here takes place in a low flow of humidified clean air. Less liquid water is used and less water vapor enters the drift tube and no additional pumping of the ion source [2] is necessary.

The drift tube is also at 10.7 hPa and consists of a stack of 7 stainless steel lenses and 8 SD Teflon spacers. The SD Teflon was either Esd500 Semitron, Flourosint 207 or 500 (Quadrant Engineering Plastics, Cincinnati OH) The 7 lenses, cathode, and curtain plate are connected via eight 10 MΩ resistors located in a slot in the spacers. The entire assembly is enclosed in an outer tube constructed of SD Teflon. Spacers and outer tubes have been constructed of both Esd500 Semitron and the Flourosint grades with similar performance. Inlet and outlet ports in the outer tube accommodate 1/4 in. (0.635 cm) OD Teflon tubing: aligned with the ports are 3.5 mm diameter holes in two of the spacers to accommodate the flow of sample gas into and out of the drift region. Either a 10 or 100 Torr

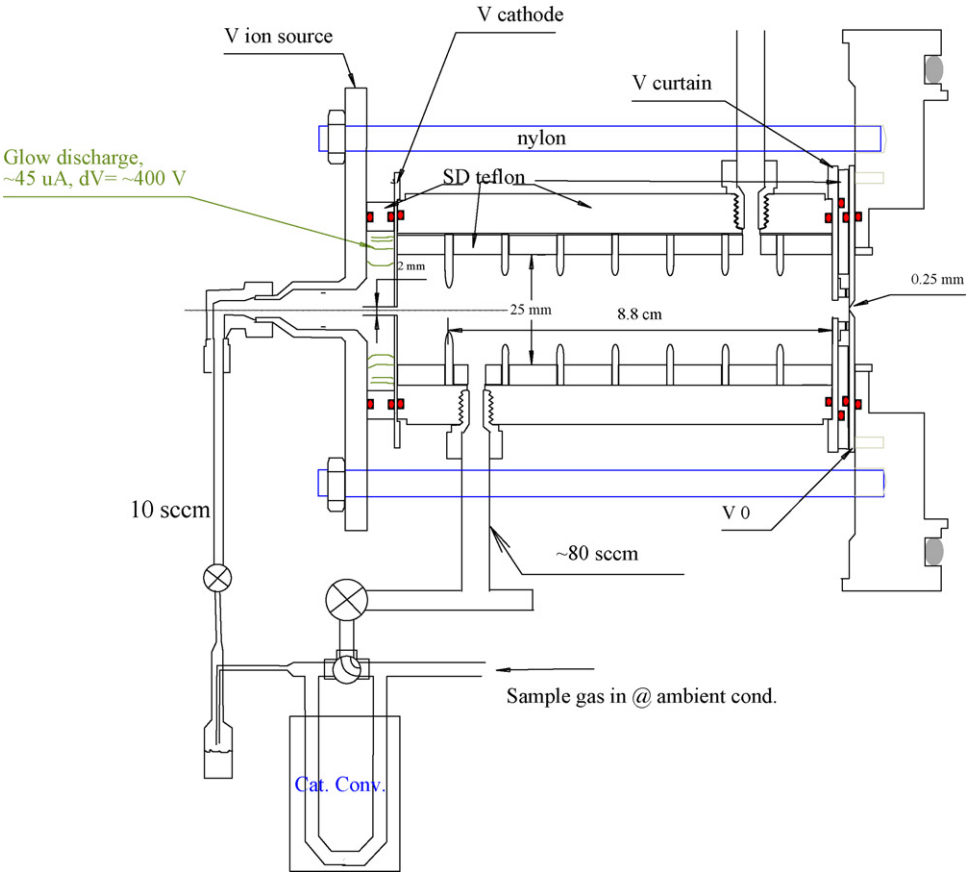

Fig. 1. Schematic drawing of sample gas inlet system, ion source, drift tube, and ion inlet for the PT-MS. Ion source is at ~3800 V, $V_{cathode}$ = ~3420 V, $V_{curtain}$ = 120 V and the ion entrance (orifice) lens V_0 = 4 V. The curtain region, just before the orifice, can be used to dry the ions by adding dry air (not done in this work). The discharge current is typically ~45 μA but S_o increased by about 100% upon increasing the discharge current to ~100 μA (voltage drop changed to ~360 V).

Please cite this article in press as: D.R. Hanson, et al., Int. J. Mass Spectrom. (2009), doi:10.1016/j.ijms.2009.01.021

capacitance manometer (Baratron, MKS) attached to the curtain region was used to monitor the drift tube pressure. There was no curtain gas flow in these studies.

The SD Teflon for the outer tube and separators has a stated resistivity of $\sim 10^{11}$ Ω cm thus the current through the SD Teflon is negligible. A voltage drop of ~3300 V is maintained across the length of the drift tube by 40–45 μA of current through the 80 MΩ resistor string. The reagent ion current, i.e, H_3O^+, measured at the orifice plate which is electrically isolated from the curtain lens, ranged from 3 to 10 nA depending upon the size of the exit hole in the cathode plate and the discharge current. A small fraction of these ions enter the mass spectrometer through the 0.25 mm orifice: approximately 1% if the reagent ion beam is a few mm in diameter.

A flow of ~10 sccm (std. $cm^3\ min^{-1}$, STP is 273 K and 1 atm) of clean air to the source is set via a stainless steel leak valve. This air is purified by sending it through a catalytic converter (see below) then humidified to ~3% water content by passing it over liquid water (~10 mL distilled, acidified with a few drops of sulfuric acid) in a small reservoir (LH side of Fig. 1).

A sample flow of ~80 sccm (up to 300 sccm) enters the drift tube in the upstream port where it combines with the source flow and reagent ions. The majority of the combined flows exits an outlet port where it passes through a large valve for regulating the drift tube pressure, and then to the roughing pump (Varian Inc., Triscroll 300). Ions and ~5 sccm of gas enter the mass spectrometer vacuum system through a 250 μm orifice. The differentially pumped vacuum system has a pressure in the first chamber of 2×10^{-4} to 6×10^{-4} Torr and the second chamber, where ions are analyzed according to mass, is typically at 1×10^{-5} Torr. The sample flow at ambient pressure is in contact with only Teflon tubing and fittings (Galtek three way solenoid valve, Entegris, Chaska, MN; PMV metering valve, Futurestar, Bloomington, MN) After the metering valve and just before entering the drift tube, the sample flow goes through a 90° turn to minimize particulates from entering the drift tube. The assembly has been in prolonged use (15 months of regular sampling of outdoor air, and intermittent high levels of VOCs in laboratory experiments) and its performance has not degraded. Reagent ion count rates are stable run-to-run with a variability of about 50% over many months. The three way solenoid valve allows for automatic zeroing of the sample air through the catalytic converter.

Sample air was zeroed by putting it in contact with platinum on alumina pellets (3.2 mm, Sigma–Aldrich) heated to ~300 °C. We found that this will destroy most, perhaps all, organic compounds that are detectable with PT-MS. de Gouw and Warneke [2] describe a similar zeroing system. This catalytic converter also provides the clean air for the source as shown in Fig. 1; the source flow keeps the catalytic converter flushed.

2.2. Calibrations

Since many uses of this type of system are quantitative, calibrations of the PT-MS are necessary. Calibrations are also useful for checking the system's performance including mass spectrometer transmission and detection efficiencies as well as to determine its sensitivity to environmental conditions such as humidity.

Known mixtures of specific compounds in air are needed and standardized gas cylinders (e.g., Taipale et al. [29], Warneke et al. [21], de Gouw and Warneke [2]) and permeation tubes (Greenberg et al. [31], Neuman et al. [32]) can be used. We used two gravimetric techniques: (i) using Henry's law of solubility as a standard and (ii) evaporation of μL amounts of dilute solutions into clean air in a glass vessel. The Henry's law method is an inexpensive way to calibrate for a wide variety of compounds whose Henry's law constants are known and we have found it to be quite reproducible. The evaporation method is actually equivalent to the standardized gas cylinder method. For both methods an advantage over the gas cylinder method is the avoidance of downstream exposure to regulators and flow meters. Methanol levels can take many hours to stabilize when passed through a regulator [2]; methanol levels using the Henry's law method stabilize in a few minutes.

Solutions in water or dodecane were prepared by serial dilution to 10^{-3} to 10^{-4} M. For the Henry's law method, a small flow (0.5–3 sccm) over solutions with solute partial pressures of 0.1 to 10×10^{-6} atm is mixed with ~100 sccm of clean air of selectable water content to get mixing ratios of 1–100 ppbv. The solutions were either at ambient temperature (21–31 °C) or held at 0 °C by immersion in ice baths. The distance between the end of the small flow inlet and the surface of the solution was 1–2 mm. Bubbling through the solution was not done to avoid a possible bias that might arise due to downstream evaporation of droplets formed upon bubble bursting.

Henry's law coefficients, H, for methanol and acetone were taken from averages of the measured values reported by Sander [13]: values for 25 °C (and those calculated for 0 °C) are 220 (1160) and 24 (110) M/atm, respectively. The uncertainty in the calibrations is dominated by uncertainties in H: on the order of 20% for methanol and acetone, the typical scatter in the literature measurements [13]. H for 3-pentanone was apparently investigated only once and the reported temperature dependency is out of line with other small ketones; the temperature dependency for acetone was also used for 3-pentanone. H for 3-pentanone at 0 and 25 °C are 20 and 90 M/atm, respectively. Uncertainty in the Henry's law constant is a drawback to this method. However, an advantage is that if values for H get better determined, the calibration accuracy will improve and even previous calibrations can become more accurate.

Mixtures in dodecane of (1) toluene, isoprene and trimethyl (1,2,4) benzene and (2) toluene, benzene, naphthalene and 3-pentanone were prepared. The Henry's law method was used to provide stable sources of these compounds in tests of changes in detection sensitivity with relative humidity. The Henry's law constants of these compounds in dodecane are not readily available, thus to get absolute calibration factors the evaporation method was used. We evaporated 1 (±0.2) μL liquid samples into a 400 cm^3 glass vessel that was continuously flushed with 120–200 sccm of clean air while the signals for the compounds were monitored. Rapid sampling by the PT-MS ensured that the net integrated signals and the flow rate would be directly related to the calibration factors for each compound. The uncertainty in this method is dominated by the ability to accurately deliver 1.0 μL of solution to the gas stream. For some compounds, the precision error is large due to interferences from dodecane vapor. A series of 6 tests for toluene were performed and we used the average of these values to get an absolute calibration factor for toluene and a measure of the precision uncertainty for this method is the standard error of the mean for these trials. The integrated signals for other compounds were then compared to that of toluene for each test to get relative calibrations. This method was also used for solutions of methanol, phenol, and cresol in water where calibrations were obtained for phenol and cresol whose Henry's law constants are not well known.

2.3. Performance: the PT-MS in use

In addition to the absolute calibration factors and their sensitivity to RH, experimental results are presented to illustrate the performance of the PT-MS. Outdoor air was sampled 15 m above ground level at Augsburg College, an urban campus situated north of a major interstate (several hundred meters) and ~3 km west of the Minneapolis downtown area. The instrument draws ~100 sccm of air down a 1/4 in. Teflon sampling line (~8 m long) that protrudes 1 m off the northwest side of the building at roofline. Periodic zeroing of the sampled air yields instrument background. Using the

Please cite this article in press as: D.R. Hanson, et al., Int. J. Mass Spectrom. (2009), doi:10.1016/j.ijms.2009.01.021

calibration factors determined here, the signals were converted to mixing ratios in ppbv (1 ppbv = 1 nmol/mol) assuming the detected ions were due to one species.

Ion breakup processes can also affect the interpretation of signals from proton transfer mass spectrometers and a few laboratory experiments for PT-MS at ~11 hPa are presented here and compared to PTR-MS studies at ~2 hPa. Compounds such as 1-dodecanol and oxalic acid that have low vapor pressures as well as other primary alcohols such as 1-butanol, 1-heptanol, and 1-octanol were investigated. A couple of biogenic compounds were also included, isoprene and geraniol. Some compounds breakup processes were investigated as a function of E/N.

3. Results

3.1. Calibrations

For the present configuration of the PT-MS—drift tube pressure and temperature (ambient and slightly heated, 45 °C), vacuum chamber pressures, lens geometry and voltages—we found 'normalized' sensitivities for compound x, S_x, of 33, 96, and 44 Hz ppbv^{-1} for methanol, acetone, and 3-pentanone, respectively. These S_x have been 'normalized' to 1 MHz of reagent ion signal by taking the actual measured sensitivities and dividing by the reagent ion signal over 1 MHz: S_o/1 MHz (see Eq. (2)). The resulting units have been termed normalized counts per second, ncps [2]. The values compare satisfactorily with the theoretical normalized sensitivities S_t determined for S_o = 1 MHz, the ion molecule rate coefficient, k, the ion drift time, t (~100 μs), and n_{1ppbv}, the concentration of analyte in the drift tube for a 1 ppbv mixing ratio in the sample flow (2.3×10^8 molecule cm^{-3}/ppbv which includes a typical flow and temperature dilution factor of 0.88):

$$S_t = f_t S_o k t n_{1ppbv} = 46\,\text{Hz/ppbv} = 46\,\text{ncps},$$
$$\text{for } k = 2 \times 10^{-9}\,\text{cm}^3\,\text{molecule}^{-1}\,\text{s}^{-1},\ f_t = 1. \quad (1)$$

f_t is the relative transmission of the product ion to the reagent ion. n_{1ppbv} depends on the ratio of source-to-sample flow and drift tube temperature, normally ~298 K.

The high sensitivity for acetone is expected according to Eq. (1) due to a large ion-molecule rate coefficient and a peak in ion transmission near 59 u. The 3-pentanone sensitivity is consistent with Eq. (1) and the expected falloff with mass in relative ion transmission. The expected sensitivity for methanol is ~20% higher than measured. Certain assumptions go into the relative transmission curve concerning the rate coefficients for PT-MS conditions, the reagent ion signal, and the ion drift time. For the measured values of S_x, S_o was taken as the sum of signals on H_3O^+ and $H_2O{\cdot}H_3O^+$ because most VOCs react fast with both of these species; a relative transmission factor of 1.15 for the latter was used in calculating S_o (see Section 3.1.2). Comparisons of measured S_x to S_t were made for low water content measurements, such that $H_2O{\cdot}H_3O^+$ signals were 5% or less of S_o. The relation between sensitivity, rate coefficients, ion drift time and relative transmission is discussed further in Sections 3.1.1 and 3.1.2.

For the Henry's law calibrations, the factor S_x was determined from the net signal (Hz) for each compound, σ_x, the partial pressure of x, P_x, in the sample flow entering the PT-MS, the ambient pressure, P_{amb}, and S_o

$$S_x(\text{ncps}) = \frac{\sigma_x(P_{amb}/P_x)(10^{-9}/1\,\text{ppbv})}{(S_o/1\,\text{MHz})} \quad (2)$$

The equation and Eqs. (1) and (3) are simplifications [34] that are very accurate for $P_x/P_{amb} \le 10^{-7}$.

Full saturation of the gas flow as it passes over the solution is assumed in measuring the sensitivity using the Henry's law method. We tested for undersaturation by including a stir bar in the vial (~1.5 cm ID) in a run and saw no significant change in signals when stirring was initiated. Undersaturation was also investigated by varying the gas flow rate through the vial. A plot of normalized signal vs. flow rate is shown in Fig. 2a showing a good linearity up to ~3 sccm. We noted some curvature to the plots at flow rates >6 and >2 sccm for calibrations with a smaller vial (ID ~0.8 cm). The onset of curvature with flow rate was dependent on the value of H: for the larger vial, departures from linearity at 6 sccm was observed at low values of H such as the ketones at ~298 K where H ~20 M/atm. For the smaller ID vial, curvature was noticeable at flow rates below 3 sccm. Fitting to a second order polynomial showed that at 1 sccm compounds were >90% saturated and calibration data was restricted to this region.

A typical run of the evaporation calibrations is shown in Fig. 2b, a plot of the signals of the compounds, and some of the ions due to the solvent dodecane, as a function of time. This method can also yield values for S_x. The net integrated signal for compound x, I_x, and the volumetric flow rate of the gas through the evaporation vessel F_g (m^3/s) are directly related to the calibration factor S_x for each compound.

$$S_x(\text{ncps}) = \frac{I_x F_g(P_{amb}/k_B T)(10^{-9}/1\,\text{ppbv})}{(N_x S_o/1\,\text{MHz})} \quad (3)$$

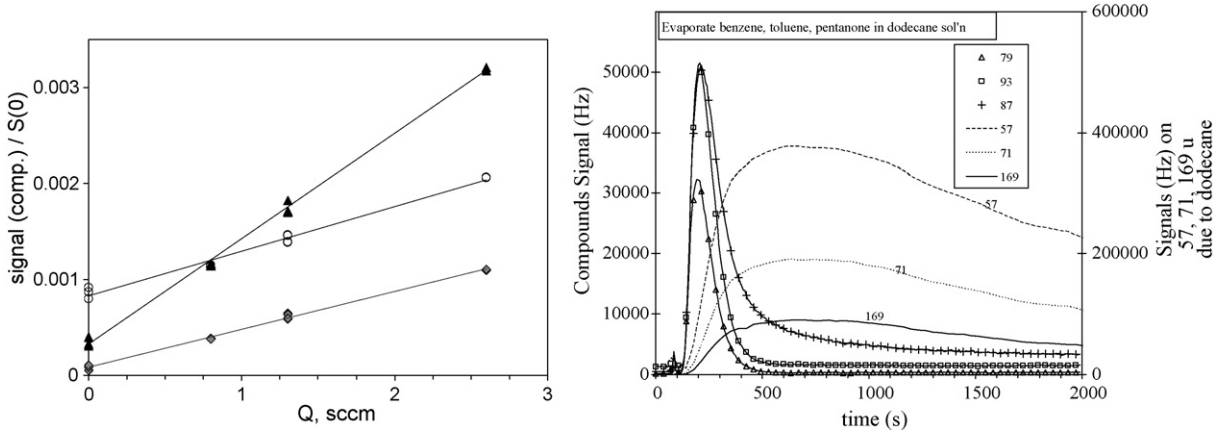

Fig. 2. (a) Henry's law calibration method. Methanol, acetone, and 3-pentanone were dissolved in water at 0 °C and signal ratios for these compounds (33, 59, and 87, respectively, divided by S_o) are plotted vs. vial flow rate. (b) Evaporation calibration method for benzene, toluene, 3-pentanone in dodecane. Note the signals on 57, 71, and 169 u that are due to dodecane (possibly impurity dodecene for 169 u).

Please cite this article in press as: D.R. Hanson, et al., Int. J. Mass Spectrom. (2009), doi:10.1016/j.ijms.2009.01.021

where k_B is Boltzmann's constant, T is ambient temperature and N_x is the number of molecules of x that were evaporated. The six trials for toluene had a standard deviation of 30% and the 95% confidence level using Student's t-test [33] is 35%. The uncertainty was heavily influenced by large departures in two of the six trials. A potential reduction in the relative error of this method can be achieved by evaporating larger (several microlitres) aliquots of solutions.

Periodic calibrations for the three compounds methanol, acetone and 3-pentanone using the Henry's law method show a good reproducibility, the average standard deviation was 9%. Earlier calibrations of a similar instrument [5] yield S_x that are uniformly higher: twice as high for acetone and isoprene, about 30% higher for methanol. The previous high sensitivities can be attributed to a higher drift tube pressure (about 25%) and to differences in lens voltages and quadrupole resolutions that affect the relative ion transmission. With the present instrument it was noted that modest (10 V) changes in the potential applied to one particular lens can increase the signal on 87 u by ~100% while the signal on 21 u decreases by ~10%: i.e., S_x for 3-pentanone increased by about a factor of two and those for methanol and acetone changed less than 20%. New calibrations of the instrument from [5] at 10.7 hPa using permeation tubes (J. Greenberg, 2008, private communication) give sensitivities for methanol, acetone, and isoprene of 40, 68, and 27 ncps, in better agreement with those reported here. The relative ion transmissions of the two nearly identical mass spectrometers are now similar.

The normalized sensitivities measured here are listed in Table 1. This includes the S_x for toluene from the evaporation experiments and the relative S_x for isoprene, benzene, trimethyl benzene, and naphthalene from these experiments. Also shown in Table 1 are theoretical sensitivities (Eq. (1)) for compounds that are routinely monitored in outdoor air using an effective relative transmission curve and certain assumptions about the temperature dependence of the ion-molecule rate coefficients (Section 3.1.2 below).

Table 1
Measured sensitivities S_x from calibrations and calculated sensitivities S_t for VOCs commonly detected in outdoor air.

Species	M·H$^+$(u)	S_x or S_t[a]	Method	Room temperature k[b]	Effective k[b]
Methanol	33	33[i]	*H*	2.5[c]	1.7
Acetonitrile	42	88	Calc	4.5[c]	3.0
Acetaldehyde	45	74	Calc	3.6[c]	2.4
Acetone	59	96	*H*	4[d]	2.7
Isoprene	69	43	ED	2	1.9
MVK, macr[e]	71	66	Calc	3.7	2.5
Benzene	79	*25*[i]	ED	2	2
Pentanone	87	44	*H*	3.4	2.3
Toluene	93	34[i]	AED	2.2[f]	2.0[g]
Phenol	95	31	EW	2.5	1.8
xylenes+	107	31	Calc	2.3[f]	2.2[g]
Cresol	109	26	EW	2.5	1.9
TMB	121	36	ED	2.4	2.4[g]
Naphthalene	129	27	ED	2.6	2.6

In all cases, yields at M·H+ were greater than 90% (E/N ~127 Td). *H* is Henry's law method, ED is relative sensitivity from the evaporated dodecane trials, EW is relative sensitivity from evaporated water trials, AED is absolute sensitivities in the evaporated dodecane method, calc are calculated sensitivities using interpolated relative transmission efficiency and ion-molecule rate coefficient.

[a] Sensitivity in ncps. S_x was measured; S_t was calculated using Eq. (1).

[b] In units of 10^{-9} cm^3 molecule^{-1} s^{-1}. Unless otherwise noted, the room temperature calculated values of Zhao and Zhang [15] were used. Note that the effective rate coefficients listed in the last column have been corrected for the high energy collisions in a PT-MS. See the text for details.

[c] Anicich [16] evaluation of measured values.

[d] Spanel et al. [17] calculated 4.0: Anicich [16] lists 3.8.

[e] MVK = methyl vinyl ketone, macr = methacrolein.

[f] Consensus of measured values quoted by Zhao and Zhang: they calculated 2.12.

[g] Within 5% of the Midey [26] values reported at 1000 K for toluene, ethylbenzene and propyl benzene.

[i] Values are RH dependent (Fig. 3b): methanol measured at sample RH = 50%, benzene measured at sample RH = 33%, and toluene measured at sample RH of ~48%.

The Henry's law method and the evaporation method were both used for some compounds. A 3-pentanone in dodecane evaporation calibration was within 20% of the Henry's law value in Table 1. For water solutions, phenol and cresol were evaporated along with methanol in water because only a few reports for their *H* values apparently exist. Comparison to data from the Henry's law method suggests that *H* for phenol in water is close to that reported in Sander's compilation [13], at 298 K 2500 M/atm, while m-cresol has a similar *H* value, about 2.5 times the value in the compilation.

3.1.1. RH dependencies

We varied the amount of water vapor in the sample air at ambient conditions to test for variations in sensitivity with relative humidity (RH). The S_x values quoted above are for relative humidities of ~30–50% at 23–31 °C for sampling air at 1 atm. S_o is the sum of signals on H_3O^+ and $H_2O{\cdot}H_3O^+$; typical values for S_o and for the isotopes for the latter (21 and 38 u) are shown in Fig. 3a. As discussed previously [5], these signals are not representative of the abundances of the proton clusters in the drift tube due to the curtain region and potential sampling issues at moderate pressures. We assume that the sum of the water proton clusters, accounting for a relative ion transmission of 1.15 for 38 u vs. 21 u, is a measure of S_o in the drift tube.

Shown in Fig. 3b are the % changes in signals with RH for methanol, isoprene, toluene, trimethyl benzene, phenol, cresol and benzene. This is the RH for the sample flow at ambient conditions, 27.8 °C and 0.985 atm. Conditions varied slightly, and RH values were scaled to the water content for RH at 27.8 °C and 0.985 atm. No significant decreases with RH were observed for any of the compounds we studied except for methanol, toluene and benzene. The lack of a humidity effect for trimethyl benzene backs up the analysis of Warneke et al. [14] that assumed no RH effect for the C8 and C9 aromatic compounds.

Changes with sample flow RH for the normalized sensitivities S_x for methanol, benzene and toluene can be calculated from the data in Fig. 3b along with ambient water content information. The RH dependent sensitivities for methanol, benzene and toluene agree with the general trends reported by de Gouw and Warneke [2,14]: a modest effect for methanol and significant effects for benzene and toluene. Their reported variation of the sensitivity at E/N = ~107 Td for toluene with RH of the sample flow agrees well with our measured variations at E/N = ~123 Td. Note that the RH dependence for toluene is also quite sensitive to E/N where the sensitivity decrease at 50% RH at 127 Td is 15% while that at 119 Td is 22%. Warneke et al. explained the RH dependencies based on equilibrium considerations of the proton water clusters and the assumption that 37 u does not react with benzene or toluene. Our results are in agreement with this reasoning as we also see linear decreases with RH. As expected, to get similar dependencies on RH as they measured for an E/N of 107 Td at 2.5 hPa, an E/N of ~120 Td is needed at 10.7 hPa. Note that for the conditions of the commercial PTR-MS (2 hPa and an E/N of 120–140 Td) there would be little if any RH dependencies to the S_x for the aromatics and methanol.

In a further refinement, de Gouw and Warneke [2,14] treat RH dependent sensitivities by using the signals for the water proton clusters as a proxy for their relative abundances in the drift tube. Doing this here is generally not possible as we have a varying E/N near the exit of the drift tube that skews the relative abundance. Theoretically calculating the relative abundances is difficult for PT-MS conditions, as shown previously [5] where the measured lifetimes of water proton clusters were much longer than experimental values under true thermal conditions. This is probably because the center of mass kinetic energy equivalent temperature is not characteristic of true thermal conditions. Furthermore, Midey et al. [26]

Please cite this article in press as: D.R. Hanson, et al., Int. J. Mass Spectrom. (2009), doi:10.1016/j.ijms.2009.01.021

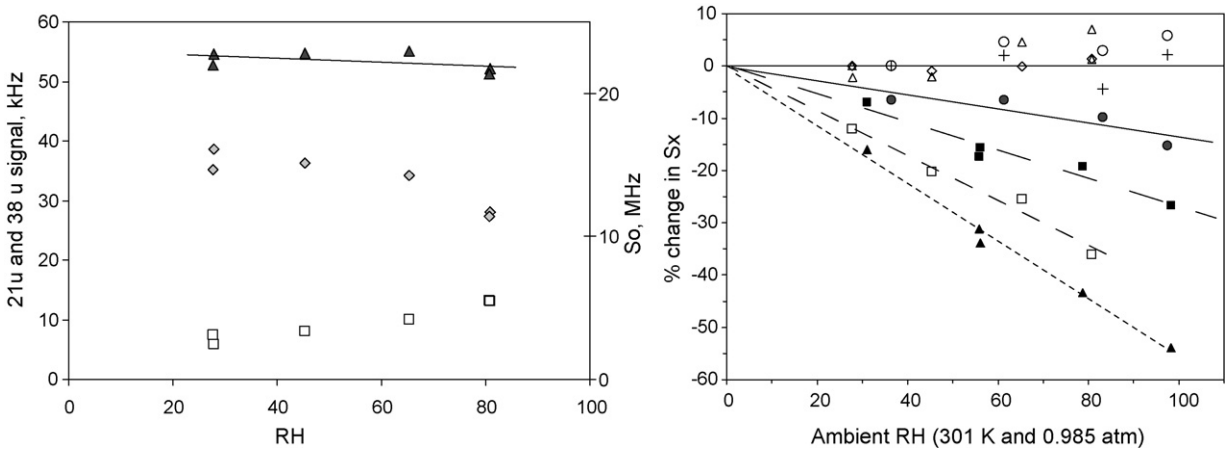

Fig. 3. Variation of (a) reagent ion signals and (b) product ion signal ratios with relative humidity of sample gas. Average conditions for sample gas are 0.985 atm and 27.8 °C; measurement RH for other conditions were adjusted to match water content. Field strength E/N = 127 Td. (a) The isotopic signals due to H_3O^+ and $H_2O{\cdot}H_3O^+$ and their sum (S_o, calculated using natural abundance ratios). (b) Variation of signals for isoprene (diamond), trimethyl benzene (open triangle), phenol (o), and cresol (+) show little dependence on RH while methanol (filled circles), toluene (filled square) and benzene (filled triangle) sensitivities decrease with RH. Measurements of toluene sensitivity changes at 119 Td (open squares) show an increased RH effect.

showed that toluene reacts with the second water proton cluster at $T \geq 500$ K nearly as fast as it reacts with the first water proton cluster. Clearly, the reasons for our observed RH dependency are not fully understood and the appropriate temperature to use for collisions in a drift tube is a source of uncertainty.

We obtained a relative sensitivity (evaporation method) of 1.35 for toluene to benzene at ~40% RH sample flow. Correcting to zero water content using Fig. 3b, the ratio is 1.24 which is somewhat lower than the 1.7 ± 0.5 ratio reported by Warneke et al. [14] for dry air and closer to a later value from this group of 1.34 [37]. A sensitivity ratio of 1.2 for these compounds was reported by Taipale et al. Taken together, these reported sensitivity ratios indicate a higher sensitivity for toluene than is given by the ratios of the ion molecule rate coefficients (1.0, see Table 1) and highlights the importance of calibrations in PT-MS work.

We observed in early runs with stainless steel fittings exposed to the sample gas at 1 atm that the signal variations with RH were non-reproducible for many compounds, particularly methanol. In some runs, the S_x for methanol appeared to increase with RH. This type of interaction between water vapor, VOCs, and sampling line materials has been noted previously ([10], D. Wiemer and J. Greenberg, private communication). Also, calibrating a PTR-MS for methanol was singled out by de Gouw and Warneke [2] as particularly difficult, presumably due to contact with inlet surface materials. Spanel and Smith [10] declined to report measured values of rate coefficients for H_3O^+ plus small alcohols because of difficulties in establishing stable concentrations.

3.1.2. Ion transmission

The relative ion sampling efficiency, ion transmission, and detection sensitivity will affect the mass spectrometer sensitivity. A relative transmission and detection sensitivity f_t for the mass spectrometer was calculated using Eq. (1), the measured S_x, t = 100 μs, and ADO theory [30] modified room-temperature values (measured and calculated) of the ion-molecule rate coefficient, k. For those species that are RH dependent (methanol, benzene, and toluene) zero water content sensitivities were determined by extrapolation. A plot of f_t vs. m/z is shown in Fig. 4 where f_t = 1 is assumed for 21 u. The relative transmission curve was iterated to obtain a final relative efficiency for 38 u vs. 21 u (1.15) as H_3O^+ and $H_3O^+{\cdot}H_2O$ ions were used for S_o.

In principle, for those species that react equally fast with H_3O^+ and $H_2O{\cdot}H_3O^+$ ions, there can be a slight increase of sensitivity with added water vapor due to an increase in reaction time as the mobility of the reagent ions decrease as they get larger with RH. This could be the reason for the slight increases (~5%) with RH of the sensitivities for several compounds shown in Fig. 3b. We did not measure ion drift times in this study. Measuring ion drift times and performing calibrations for compounds such as acetaldehyde and acetonitrile would improve the relative transmission curve and the RH-dependent sensitivities.

A suggested by a reviewer the room temperature values for k were corrected to account for the high energy collisions in the ion drift tube. An effective temperature, 1200–1600 K [27], based on the center of mass translational kinetic energy, was used along with the temperature dependence to k given by Su and Chesnavich [33] to obtain the change in k from 300 K values. These changes ranged from −40 to −48% for the polar species, and 0 to −10% for the non-polar species using the effective temperature. Because there is less energy in the collision than this effective temperature implies due to the rotationally cold reactant neutral, we arbitrarily adopted a factor of 67% of the change to use in Table 1. This factor affects our determination of the relative transmission curve however the same factor is used in reverse so that biases in S_t should be less.

3.1.3. Sensitivities, discharge parameters, curtain region

Calculated S_t for compounds that we monitor in outdoor air but are not calibrated for are also listed in Table 1. S_t was calculated from Eq. (1), the transmission curve shown in Fig. 4, and the temperature-corrected ion-molecule rate coefficients (last column) in Table 1. An

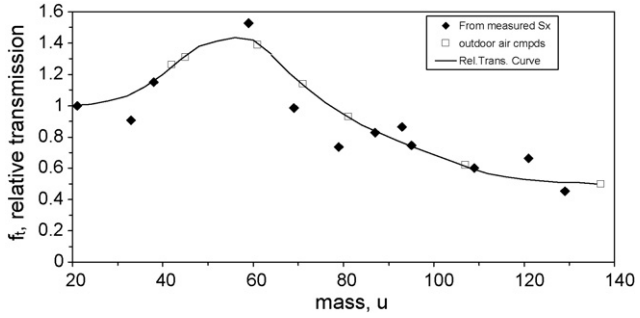

Fig. 4. Relative ion transmission and detection efficiency as a function of mass where f_t at 21 u is taken to be unity. The solid curved line is an estimate of the relative transmission as a function of mass. The f_t for typical outdoor air compounds not calibrated for are indicated by open squares.

Please cite this article in press as: D.R. Hanson, et al., Int. J. Mass Spectrom. (2009), doi:10.1016/j.ijms.2009.01.021

uncertainty of ~20% is estimated in the S_t which is characteristic of the general scatter of the measured S_x about the transmission curve in Fig. 4. The transmission efficiencies of isoprene and benzene are somewhat low, especially in comparison to that for toluene and TMB. There may be a small bias in our calibration methods for these two compounds and in future calibrations we will use volumetric in addition to gravimetric quantification. The sensitivity ratio of benzene to toluene is in agreement with other PTR-MS work, suggesting that additional investigation of these ion-molecule reaction rates is also needed.

It has been emphasized [1,2] that proton mass spectrometers are best deployed as gas monitors and are not intended for gas analysis because many compounds can give the same mass ion. Fortunately, many atmospheric compounds can be assigned to unique m/z as shown by de Gouw et al. [34]. Noting that most ion molecule reaction rates fall within 20% of that given in Eq. (1) and assuming that fragmentation is small, many compounds can be given a rough mixing ratio by using the S_t or S_x for a compound near to it in detected mass. When discussing the mixing ratio of a possible compound that contributes to the signal at a designated m/z a designation of ppbv* will be used subject to these assumptions.

With the glow discharge ion source operated at ~45 μA, the reagent signal S_o (H_3O^+ plus hydrates) is typically 15–30 MHz, and a typical sensitivity is 0.5–1 Hz per pptv. Reagent ion signal is dependent on the size of the hole in the source exit plate (cathode) and also on the discharge current. As noted in Fig. 1 caption, a doubling of the glow discharge current roughly doubles S_o which would double the sensitivity but not necessarily double detection limits due to increases also in backgrounds. Note that low abundance isotopes are monitored for the species H_3O^+ and $H_2O{\cdot}H_3O^+$.

For an instrument that had been sampling air for several days in winter, the major 'impurity' ions and typical background levels and detection limits for commonly detected VOCs are listed in Table 2. A 50% duty cycle detection limit $DL_{50\%}$ as a function of measurement time $t_m = 5$ s for both sample and background (50% duty cycle), is given by

$$DL_{50\%} = B + (B^2 + 4B\text{ppb}_o)^{0.5} \quad (4)$$

where $B = 3^2/(2(S_o/1\,\text{MHz})S_x t_m)$, 3 is the signal-to-noise ratio desired, and ppb_o is the equivalent mixing ratio of analyte for the background signal. It yields comparable detection limits to the equation presented by de Gouw et al. [37]; it gives higher values when background levels are low. Detection limits are generally about a factor of two better than those reported by de Gouw et al. [37] for similar t_m even though background signals as a percent of S_o are comparable; this is due to a higher sensitivity and a lower value for B in Eq. (4). Background signals for 30, 46 and 47 u are very high for the present instrument. NO^+ and NO_2^+ are made in the source (30 and 46 u) due to the presence of air and 47 u is most likely due to N_2 clustering with H_3O^+ upon entering the vacuum system.

The curtain region electric field is on average about 5% greater than the electric field E in the drift tube (typically ~330 V/cm). Its geometry leads to a peak in the electric field near the orifice of about 15% over the drift tube E. The ions spend about 1 μs in this region; both ion fragmentation patterns and proton water cluster distributions can be affected. An alternate orifice arrangement that does not have a curtain region was also used in the course of these studies and there were no significant differences in sensitivities from those for the apparatus shown in Fig. 1.

Table 2
Rough signal levels for major impurity ions and equivalent backgrounds in ppbv for analytes of interest in winter.

Mass	Identity	Background (% of S_o)	Note, ppbv*	$DL_{50\%}(t_m)$, ppbv
30	NO^+	1.5–3		–
32	O_2^+	0.3	RH dep.	–
33	$O^{17}O^{16+}$, CH_3OH	0.007	2	0.11
37	$H_2O{\cdot}H_3O^+$	1–50	RH dep.	–
41	Breakup ion, etc.	0.0004	0.1	–
43	Fragment, propene	0.008	2	–
45	Acetaldehyde,CO_2H+?	0.026	3.5	0.09
46	NO_2^+, $CO_2H_2^+$?	0.3		–
47	$N_2{\cdot}H_3O^+$	0.7	RH dep.	–
59	Acetone	0.008	0.8	0.04
69	Isoprene/furan,	0.0003	0.07	0.018
71	MVK/macr	0.0002	0.04	0.009
79	Benzene	0.0004	0.08	0.034
93	Toluene	0.0001	0.03	0.014
107	Xylenes, etc.	0.00003	0.01	0.010
121	TMB, etc.	0.00006	0.015	0.010
135	Aromatic	0.000017	0.005	0.007
137	Monoterpene	0.000013	0.009	0.015

Ions at 55 and 73 u are dominated by water proton clusters and are ~0.5% and 0.01%, respectively, of S_o. The 10 s theoretical detection limit (Eq. (4)) for a typical $S_o = 20$ MHz is for two 5 s measurements: sample and background. ? means tentatively assigned.

3.1.4. Outdoor air

Shown in Fig. 5a are measurements over 15 months of methanol ($m/z = 33$ u), acetaldehyde (45 u) and acetone (59 u). Fig. 5b shows isoprene (69 u), MVK/macr (71 u), acetonitrile (42 u) and the aromatic compounds (79, 93, 107, 121 u). The data are 1–4 day averages of ~0.5 s data. Among the aromatics, benzene has a peak in winter, which could be due to a higher influence of combustion sources in winter such as furnaces and traffic. The ratio of toluene to benzene changes from about unity in the winter to about 2 in the summer. A summertime emission ratio of ~4 for these compounds was inferred from observations in Boston and New York in 2002 and

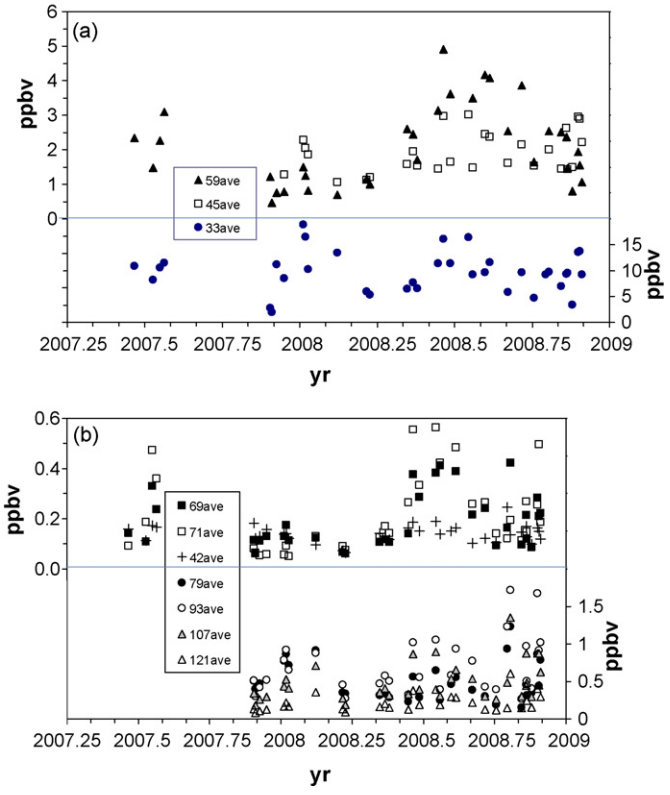

Fig. 5. Long-time averages of selected VOC mixing ratios (ppbv) in outdoor air periodically sampled over 15 mos. (a) Methanol (33 u, lower right scale), acetaldehyde (45 u), and acetone (59 u). (b) Isoprene* (69 u) and [MVK + macr]* (71 u), acetonitrile (42 u) and the aromatic compounds (79–121 u, lower right scale).

2004 [21]. These ratios are likely to be dependent on source types at these urban sites.

There are annual cycles for acetone, isoprene and MVK + macr where peaks in summer are apparent. The peaks in the latter two are in line with the cycles in biogenic activity. There is not a discernible annual cycle for methanol, acetaldehyde and acetonitrile. Note that acetaldehyde may be influenced by artifacts [2]. Methanol levels average 10 ppbv throughout the year suggesting that anthropogenic sources in winter balance the expected declines in biogenic production. There are times in spring and fall where all the VOCs are at a minimum. This is probably influenced by meteorological conditions and also the changeover between wintertime (anthropogenic) and summertime (biogenic) sources.

In winter, the signals on mass 69 u (usually attributed to isoprene) and 71 u (usually attributed to MVK + macr) often are well correlated to benzene signals. These compounds (in ppbv*) are plotted vs. benzene in Fig. 6a (December 2007, average temperature −8 °C, windspeeds averaged 5 mph) and comparable measurements during the summer (June 2008, ave. T = 21 °C, windspeeds average 10 mph) are shown in Fig. 6b. Both sets of data are 0.5 s dwell time every 10 s for ~20 h. In wintertime when biogenic sources are believed to be negligible, the correlation of benzene and VOCs at 69 u (isoprene, furan), and 71 u (MVK, methacrolein, perhaps pentene) suggest a common source. These observations of [compounds] at 69 u (average of 0.1 ppbv*) and 71 u (average of ~0.05 ppbv*) suggest that they are approximately 15 and 8% of [benzene], respectively (ppbv* is discussed in Section 3.1.3) Isoprene is known to have automobile or industrial sources [19,20] while pentenes can be detected on 71 u. Warneke et al. [21] observed pentenes to comprise 20% or more of benzene emissions in an urban environment. Anthropogenic sources are a likely explanation for our observations of the signals on 69 u and 71 u during winter.

This contrasts with observations in the summer (Fig. 6b) where benzene and the biogenic compounds isoprene and MVK + methacrolein are related differently. Even in the late spring data shown in the figure, there is a much larger contribution of biogenic compounds than in winter. Note that 69 and 71 u are at average levels of 0.13 and 0.22 ppbv* while benzene averages 0.2 ppbv during this time period. Data taken later that summer (July 2008) show much higher levels of 69 and 71 u indicating average levels of isoprene and MVK of ~0.5 ppbv*.

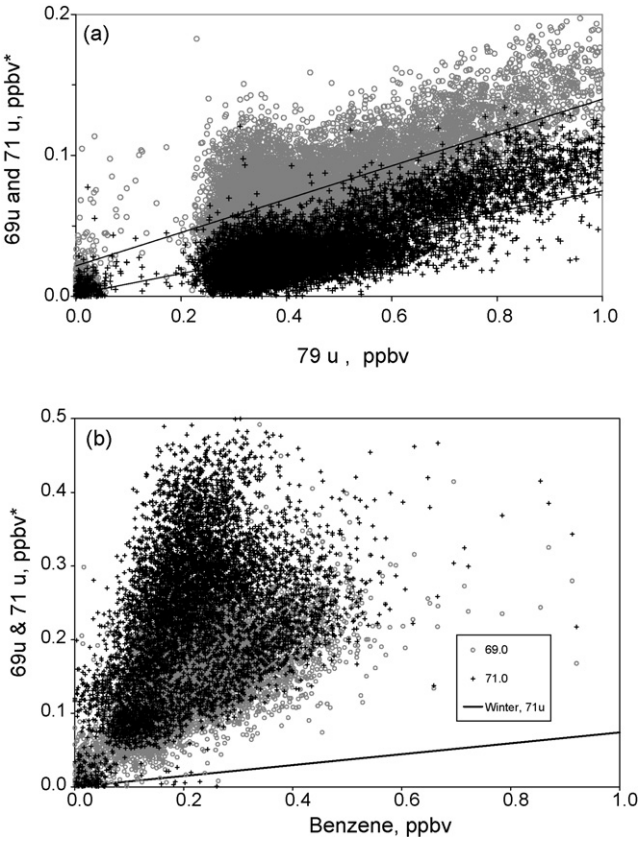

Fig. 6. Isoprene* and MVK* (3.1.3), masses 69 and 71 u, vs. benzene (79 u) (a) for one day in winter 2007 and (b) one day in summer 2008. Summertime compounds at 69 and 71 u are likely to be isoprene and MVK + methacrolein, respectively, while wintertime 71 u is likely to be pentene and other alkenes.

3.1.5. Mass spectrums of outdoor air

Shown in Fig. 7 are mass spectrums of outdoor air in winter (1 s dwell time per mass) with scans of the instrument background (1 s dwell) subtracted. The aromatic compounds detected at 79, 93, 107, 121, and 135 u are strongly indicated. Prominent peaks at 61 and 73 u are likely due to acetic acid and methyl ethyl ketone, respectively. Commonly observed peak sequences at 81–83–85–87 u, 97–99–101 u, and 117–119 u indicate substances present in the 50–100 pptv* range. Williams et al. [22] showed scans of PTRMS forest air data and assigned some of these peaks to biogenic compounds. In urban wintertime, anthropogenic unsaturated species probably contribute significantly: e.g., 81, 83, 85 could be various C6 species, 95–101 various C7 species and 117

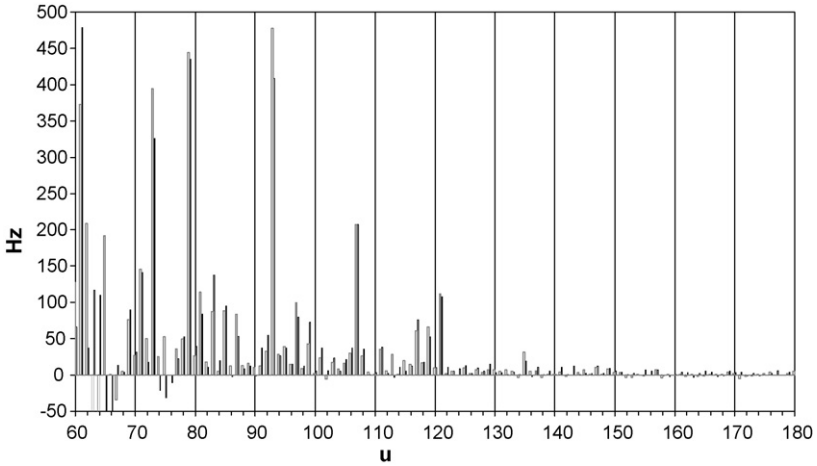

Fig. 7. Net signals at masses from 60 to 160 u from outdoor air sampled in January. Assuming no ion breakup processes, a signal of 1 Hz is roughly equal to a mixing ratio of 2 pptv* (pmol/mol, see Section 3.1.3 for * designation).

Please cite this article in press as: D.R. Hanson, et al., Int. J. Mass Spectrom. (2009), doi:10.1016/j.ijms.2009.01.021

and 119 various C9 species. They could also be due to ion breakup processes. Many other peaks due to compounds in the few pptv* range are noticeable above the background level.

These mass spectrum are shown from 60 u and higher because instrument background count rates are low (< a few hundred Hz up to ~80 u, <10 Hz near 100 u, and a few Hz at >120 u). Identifying the compounds responsible for these signals is necessary; such as measurements in conjunction with a gas chromatographic analysis system [36]. These mass spectrums show a reproducible 1 s detection of compounds that approach the single digit pptv* level in this mass range (subject to the assumption of known or little fragmentation).

3.2. Ion breakup processes

An important VOC sampling issue for the PT-MS is ion fragmentation processes. We present fragmentation experiments for a set of n-alcohols, isoprene and one dicarboxylic acid. Compounds were sampled by dynamic dilution of their vapor pressures or by evaporation of small amounts into clean air in a glass vessel. RH in the sample flow was between 25 and 50% except for oxalic acid which was 5–10%. Oxalic acid vapor level after several hours of flow had not stabilized but was high enough to be monitored with PT-MS.

Note that the product ions for all the species in the calibration experiments were the $M{\cdot}H^+$ ions (Table 1, fragmentation <10% for typical E/N of 127 Td). In the course of the isoprene studies, we varied the E/N from 127 to 140 Td and noted that the 41 and 39 u fragments increased from about 1 and 3%, respectively, of the 69 u ion to about 12 and 25%, respectively, at 140 Td.

Protonation of alcohols such as phenol and methanol and subsequent drift at an E/N of 120–130 Td does not lead to significant fragmentation of $M{\cdot}H^+$. As has been reported previously in PTR-MS work at 2 hPa [11,23,28], protonation of other alcohols results in primarily fragment ions, (E/N was unfortunately not specified nor apparently varied in Refs. [11,23,28]). The fragmentation patterns of isoprene, the alcohols, and oxalic acid (as a function of E/N) are presented in Table 3. We also investigated fragmentation of 1-octanal at a variety of E/N, also shown in Table 3.

The general butanol fragmentation pattern (majority 57 u) is consistent with that reported by Spanel and Smith [10] however we detected <0.5% on the parent ion. Spanel and Smith investigated alcohols including hexanol and octanol and observed increasing fragmentation with carbon number at ambient temperatures. The detailed fragmentation patterns they report does not apply to our observation that 57 u is the dominant ion in almost all cases. The ion-molecule collision in a PT-MS drift tube is characteristic of a temperature of 1000–2000 K [27] much different than the ~room temperature conditions of a selected ion flow tube mass spectrometer. Product ions in a PT-MS are also in a somewhat hostile environment and would be subject to fragmentation. This is consistent with our results for decreasing fragmentation with E/N for 1-octanol.

Fragmentation patterns in the PT-MS at 10.7 hPa are qualitatively similar to those observed at 2 hPa. Buhr et al. [28], Boscaini [23] and Fall et al. [11] report ion breakup patterns in a PTR-MS for several alcohols and significant amounts of signal at 57 u were observed for: 1-butanol, methylpropanol, 1-hexanol, ethylhexanol, 2-nonanol. Spanel and Smith [10] report significant 57 u signal for 1 and 2 octanol at room temperature, also consistent with our observation. Boscaini report a geraniol fragmentation pattern that is similar to that shown in Table 3, with 81 u dominant, followed by 137 u with only about 2% on $M{\cdot}H^+$(155 u).

In general for the high energy conditions of an ion drift tube at E/N ~120 Td, the most prevalent fragment ion for the alcohols was 57 u, presumably $C_4H_9^+$, and a common ion was at 41 u, possibly $C_3H_5^+$. E/N was lowered to 80 Td or less for 1-butanol with little influence on the fragmentation patterns. As phenol, geraniol, and hexenol [11] do not produce this ion, it seems that multifunctional alcohols are protected from fragmentation to 57 u, as suggested by Boscaini [23].

Fragmentation of oxalic acid is an interesting case because it is dominated by an even numbered (in u) mass fragment. At an E/N setting of 127 Td, there was no or very little indication of any signal at $M{\cdot}H^+$ (91 u) or its dehydrate, however signal at 46 u, possibly $CO_2H_2^+$, was quite noticeable above the high background. Lowering the E/N to ~100 Td increased the signal on 91 u by orders of magnitude: it became comparable to the signal on m/z = 46. The signals on 46 u were at most 10% of the background signal and the fragmentation pattern shown in Table 3 should be considered in this light. Oxalic acid is the only non-N containing species that we have studied that leads to significant signal at an even atomic mass unit. Ervasti et al. [35] studied the fragmentation of protonated oxalic acid and also observed a significant ion fragment at 46 u.

3.3. PT-MS and circular glow discharge vs. conventional PTR-MS

The main advantage of an ion drift tube at high pressure is the high number density of reactant at a given mixing ratio thus leading to high sensitivity S_x through a high n_{1ppbv} value in (Eq. (1)). A limitation to increasing the pressure is that a high E is needed to maintain an E/N of ~120 Td, potentially stressing insulating materials such as the SD Teflon. When the previous system [5] was operated at 13 hPa over time periods of months, S_o became quite variable, sometimes decreasing by 80% and the drift tube was susceptible to discharges. This decrease in reliability was presumably due to contamination of SD Teflon surfaces over time. A lower E at

Table 3
Ion fragmentation of some selected VOCs, primarily alcohols. Patterns as observed in %: no transmission effects were included.

Compound ($M{\cdot}H^+$)	E/N	$M{\cdot}H^+ - H_2O$	$M{\cdot}H^+$	$M{\cdot}H^+ + H_2O$	57 u	41 u	43 u	71 u	Other fragments
Butanol (75 u)	125	>90	<0.5		>90	~10			
Heptanol (117 u)	125	<1	<0.5		~90	~5			97 u: ~5
Octanol (131 u)	125	1	~0.02	<0.1	50	9	21	28	
.	112	9	0.1	1	39	0.6	7	46	
.	99	30	0.7	15	19	<0.1	0.7	31	167 u: 5
dodecanol (187 u)	125	4	< 0.5	<1	52	7	20	9	97 u: 5, 115 u: 2.5
oxalic acid (91 u)	122		~4						46 u: 95
	116		~10	~2					46 u: 88
	105		~30	25					46 u: 50, 117 u: 5
	94		~15	45					46 u: 40, 117 u: 10
Geraniol (155 u)	125	16	~1		2	12			81 u: 44, 95 u: 15
Isoprene (69 u)	127		96			3			39 u: 1
	140		75			17			39 u: 8

Butanol, heptanol, octanol, dodecanol, and oxalic acid were 98% pure or better (Sigma–Aldrich). Note that E/N is given for the electric field in the drift tube: the E in the curtain region can reach to 15% higher for 1–2 μs of transit time.

Please cite this article in press as: D.R. Hanson, et al., Int. J. Mass Spectrom. (2009), doi:10.1016/j.ijms.2009.01.021

the lower *N* here is probably one of the reasons that the PT-MS used at 10.7 hPa has good performance over many months. There are also twice as many lenses in the drift tube in the present system.

The advantages of the circular glow discharge presented here are (i) ease of ignition at ~11 hPa where generally it starts up when 1–1.5 kV is applied to the anode, (ii) a low discharge current of ~45 μA gives a good sensitivity: ~1 Hz/pptv for many compounds, (iii) sensitivity can be increased by raising the discharge current (see Fig. 1 caption), (iv) ease of construction and assembly, and (v) much lower flow rates of water for the source are needed.

A drawback of the PT-MS as deployed here is the high backgrounds at 45, 46, and 47 u in comparison to PTR-MS. This compromises measurements of acetaldehyde, C2 amines, formic acid and ethanol. While all the sources of these ions in the PT-MS are not known, deploying an ion preparation chamber, such as the secondary chamber of the PTR-MS ion source, will probably help decrease ions at 45, 46, and 47 u. Also, as discussed recently, Lindinger et al. [36] replaced elastomer materials, such as o-rings, with Teflon conflat-type connections and they noted a substantial decrease in background count rates.

4. Summary

The use of a circular glow discharge as the ion source on a custom PT-MS at 10.7 hPa was described and work designed to further characterize the detection of VOCs using this technique was presented. Also, typical uses of the instrument were demonstrated and its performance is comparable to the conventional PTR-MS instruments. This work builds on a previous instrument [5,6], where a radioactive source was employed.

Data from sampling outdoor air over 15 mos was presented and demonstrated the reliability of the system. In wintertime, it was confirmed that there is likely to be anthropogenic contributions to signals at mass 69 and 71 u. Theoretical detection limits (5 s) are as low as 20 pptv for many compounds.

Calibrations of the PT-MS were based on gravimetrically prepared solutions, using either Henry's law or evaporation of microliter amounts of the solutions. A relative transmission curve for the instrument was presented. Significant water dependencies for benzene and toluene were found and these dependencies are consistent with earlier work.

Ion breakup processes were investigated and 57 u was a dominant ion from straight chain alcohols of 7 carbon and larger. A very interesting finding was the contribution of an even mass (46 u) fragment ion from the reaction of water–proton clusters with oxalic acid.

Acknowledgements

The comments of the reviewers were very helpful in revising the manuscript. Conversations with J. de Gouw, C. Warneke, T. Karl and J. Greenberg are gratefully acknowledged. This work was supported by the URGO program of Augsburg College, by grants from the Minnesota Space Grant College Consortium and The Eppley Foundation for Research to Augsburg College, and by National Science Foundation grant ATM-0301213.

References

[1] W. Lindinger, A. Hansel, A. Jordan, Int. J. Mass Spectrom. Ion Processes 173 (1998) 191.
[2] J. de Gouw, C. Warneke, Mass Spectrom. Rev. 26 (2007) 223.
[3] A. Hansel, W. Singer, A. Wisthaler, M. Schwarzmann, W. Lindinger, Int. J. Mass Spectrom. 267 (2007) 697.
[4] T. Karl, A. Guenther, Int. J. Mass Spectrom. 239 (2004) 77.
[5] D. Hanson, J. Greenberg, B.E. Henry, E. Kosciuch, Int. J. Mass Spectrom. 223–224 (2003) 507.
[6] D. Hanson, J. Orlando, B. Noziere, E. Kosciuch, Int. J. Mass Spectrom. 239 (2004) 147.
[7] G. Francis, Gas Discharges II, v. XXII, Encyclopedia of Physics, 1956.
[8] A. Anders, S. Anders, Plasma Sources Sci. Technol. 4 (1995) 571.
[9] E.H. Daughtery, W.W. Harrison, Anal. Chem. 47 (1975) 1024.
[10] P. Spanel, D. Smith, Int. J. Mass Spectrom. 167/8 (1997) 375.
[11] R. Fall, T. Karl, A. Hansel, A. Jordan, W. Lindinger, J. Geophys. Res. 104 (1999) 15963.
[12] A. Tani, S. Hayward, C.N. Hewitt, Int. J. Mass Spectrom. 223–224 (2003) 561.
[13] R. Sander, Henry's Law Constants, in: NIST Chemistry WebBook, NIST Standard Reference Database Number 69, P.J. Linstrom, W.G. Mallard (Eds.), National Institute of Standards and Technology, Gaithersburg, MD 20899, June 2005 (http://webbook.nist.gov).
[14] C. Warneke, C. van der Veen, S. Luxembourg, J.A. de Gouw, A. Kok, Int. J. Mass Spectrom. 207 (2001) 167.
[15] J. Zhao, R. Zhang, Atmos. Environ. 38 (2004) 2177.
[16] V.G. Anicich, J. Phys. Chem. Ref. Data 22 (1993) 1469.
[17] P. Spanel, Y. Ji, D. Smith, Int. J. Mass Spectrom. 165/6 (1997) 25.
[19] A. Borbon, H. Fontaine, M. Veillerot, N. Locoge, J.C. Galloo, R. Guillermo, Atmos. Environ. 35 (22) (2001) 3749.
[20] S. Reimann, P. Calanca, P. Hofer, Atmos. Environ. 34 (2000) 109.
[21] C. Warneke, S.A. McKeen, J.A. de Gouw, P.D. Goldan, W.C. Kuster, J.S. Holloway, E.J. Williams, B.M. Lerner, D.D. Parrish, M. Trainer, F.C. Fehsenfeld, S. Kato, E.L. Atlas, A. Baker, D.R. Blake, J. Geophys. Res. 112 (2007) D10S47, doi:10.1029/2006JD007930.
[22] J. Williams, U. Poschl, P.J. Crutzen, A. Hansel, R. Holzinger, C. Warneke, W. Lindinger, J. Lelieveld, J. Atmos. Chem. 38 (2001) 133.
[23] E. Boscaini, Ph.D. thesis, University of Innsbruck, Innsbruck, Austria, 2002.
[26] A.J. Midey, S. Williams, S.T. Arnold, A.A. Viggiano, J. Phys. Chem. A 106 (2002) 11726.
[27] A.A. Viggiano, R. Morris, J. Phys. Chem. 100 (1996) 19227.
[28] K. Buhr, S. van Ruth, C. Delahunty, Int. J. Mass Spectrom. 221 (2002) 1.
[29] R. Taipale, T.M. Ruuskanen, J. Rinne, M.K. Kajos, H. Hakola, T. Pohja, M. Kulmala, Atmos. Chem. Phys. Discuss. 8 (2008) 9435.
[30] T. Su, W.J. Chesnavich, J. Chem. Phys. 76 (1982) 5183.
[31] J.P. Greenberg, H. Friedli, A.B. Guenther, D. Hanson, P. Harley, T. Karl, Atmos. Chem. Phys. 6 (2006) 81.
[32] J.A. Neuman, T.B. Ryerson, L.G. Huey, R. Jakoubek, J.B. Nowak, C. Simons, F.C. Fehsenfeld, Environ. Sci. Technol. 37 (13) (2003) 2975.
[33] H.L. Youmans, Statistics for Chemistry, Charles E. Merrill Publishing, Columbus OH, 1973.
[34] J. de Gouw, C. Warneke, T. Karl, G. Eerdekens, C. van der Veen, R. Fall, Int. J. Mass Spectrom. 223 (2003) 365.
[35] H. Ervasti, R. Lee, P.C. Burgers, P.J.A. Ruttink, J.K. Terlouw, Int. J. Mass Spectrom. 249–250 (2006) 240.
[36] C. Lindinger, P. Pollien, S. Ali, C. Yeretzian, I. Blank, T. Mark, Anal. Chem. 77 (2005) 4117.
[37] J.A. de Gouw, P.D. Goldan, C. Warneke, W.C. Kuster, J.M. Roberts, M. Marchewka, S.B. Bertman, A.A.P. Pszenny, W.C. Keene, J. Geophys. Res. D 108 (2003) 4682.